Supplementary Figures

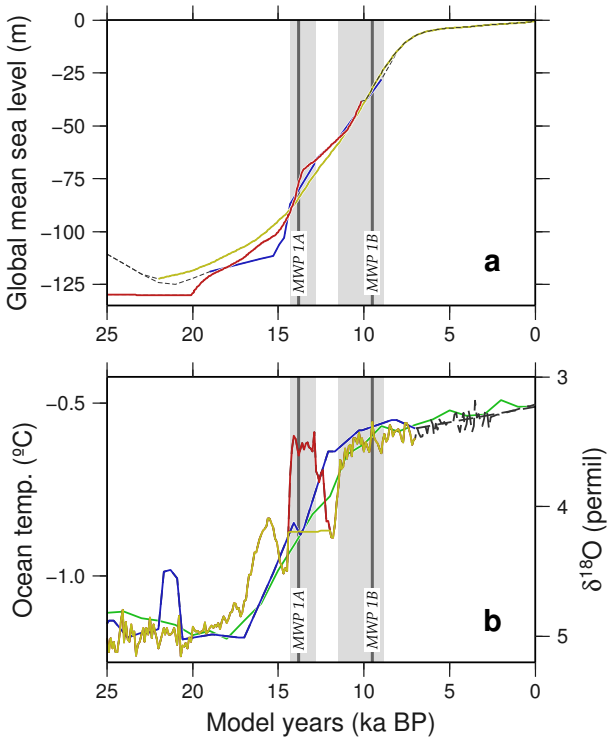

Supplementary Figure 1 | Time-series forcings used to drive the experimental ensemble. a: sea-level curves from Refs 1 (blue), 2 (yellow), and 3 (red), and **b:** ocean-temperature trends from a global benthic δ^{18}O stack[4] (green), the Southern-Ocean benthic δ^{18}O record from Ocean Drilling Program (ODP) leg 181, site 1123 (Ref. 5, blue), and two mid-depth (485-700 m) temperature trends from the LOVECLIM model, with (FWF, red) and without (NFW, yellow) a prescribed Antarctic meltwater pulse from 14.4-12.4 ka BP (Ref 6). Vertical grey bands indicate timings of meltwater pulses 1A and 1B (Ref 2).

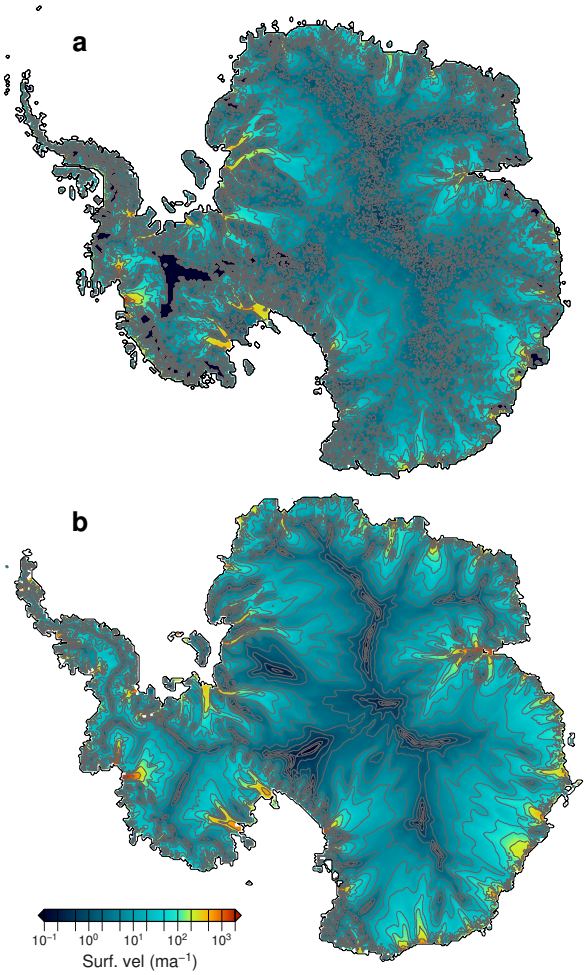

Supplementary Figure 2 | Comparison of present-day grounded ice extent and surface velocity. a: Interferometric Synthetic Aperture Radar-derived surface velocity[7] and **b:** ensemble-mean modelled surface velocity (this study). Modelled ice volume is within 2% of the value inferred from the latest compilation of ice thickness data[8].

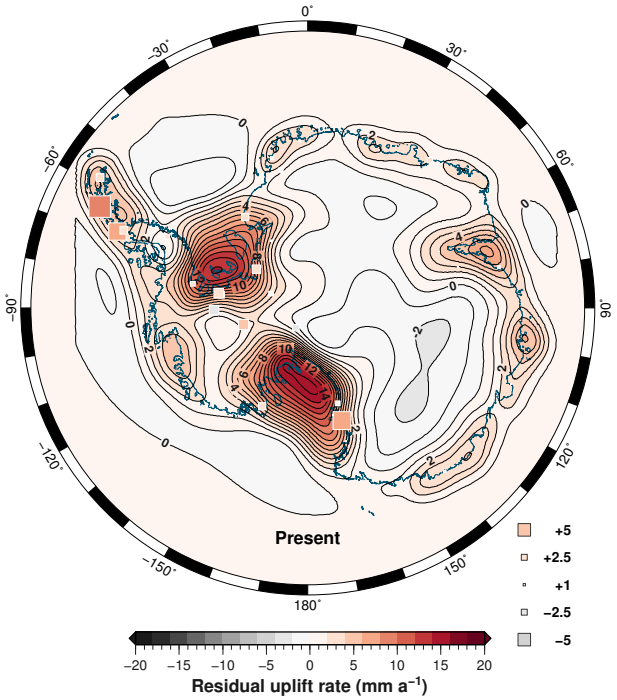

Supplementary Figure 3 | Residual uplift simulated by our model ensemble. Greatest rebound occurs in the Weddell and Ross embayments, whereas parts of East Antarctica are characterised by slow subsidence. GPS-derived uplift measurements from Ref. 9 also shown (colour-coded squares).

Supplementary Tables

Parameter	Value	Units
Domain resolution (x, y)	15	km
Ice grid resolution (z)	0.024	km
Bedrock grid resolution (z)	0.1	km
Run length	50000	year
Spatial output interval	100	year
Timeseries output interval	1	year
Air temperature lapse rate	0.0075	$^{\circ}m^{-1}$
Palaeprecipitation exponent	0.068	-
SIA enhancement	2.85	-
SSA enhancement	0.7	-
Till porewater fraction	0.8	-
Density of lithosphere	3300	kg m^{-3}
Flexural rigidity	5×10^{24}	Nm
Viscosity of mantle	1×10^{21}	Pa s

Supplementary Table 1 | Parameter values used for the suite of model runs that best fit the empirical constraints.

Ice Core	Lon (°E)	Lat (°S)	LGM change	Method of inference	Source
EPICA DML	0	75.00	-100 to +60	Modelling	Ref. 10
Berkner Isl.	-45.70	79.57	+1400	Modelling	Ref. 11
WAIS Divide	-112.09	79.47	+200	Modelling	Ref. 12
Byrd Station	-119.52	80.02	+200	Modelling	Ref. 13
Siple Dome	-148.82	81.67	+200 to +400	Modelling	Ref. 14
Roosevelt Isl.	-161.99	79.42	unknown	-	-
Taylor Dome	158.72	77.80	<+50	Geologic data	Ref. 15
DOME F	39.70	77.32	-120	Modelling	Ref. 16
Vostok	106.83	78.47	-100	Total gas	Ref. 17
DOME C	123.00	75.00	-120	Modelling	Ref. 16
Law Dome	112.82	66.78	+136 to +335	Total gas	Ref. 18
Talos Dome	159.18	72.82	unknown	-	-

Supplementary Table 2 | Ice cores used as model constraints, showing relative changes at LGM and basis of inference.

Supplementary References

[1] Deschamps, P., Durand, N., Bard, E., Hamelin, B., Camoin, G., Thomas, A. L., Henderson, G. M., Okuno, J., and Yokoyama, Y. Ice-sheet collapse and sea-level rise at the Bølling warming 14,600 years ago. *Nature* **483**, 559–564 (2012).

[2] Stanford, J., Hemingway, R., Rohling, E., Challenor, P., Medina-Elizalde, M., and Lester, A. Sea-level probability for the last deglaciation: A statistical analysis of far-field records. *Global and Planetary Change* **79**, 193–203 (2011).

[3] Clark, P. U., Dyke, A. S., Shakun, J. D., Carlson, A. E., Clark, J., Wohlfarth, B., Mitrovica, J. X., Hostetler, S. W., and McCabe, A. M. The Last Glacial Maximum. *Science* **325**, 710–714 (2009).

[4] Lisiecki, L. E. and Raymo, M. E. A Pliocene-Pleistocene stack of 57 globally distributed benthic δ^{18}O records. *Paleoceanography* **20**, PA1003,17 PP. (2005).

[5] Elderfield, H., Ferretti, P., Greaves, M., Crowhurst, S., McCave, I., Hodell, D., and Piotrowski, A. Evolution of ocean temperature and ice volume through the Mid-Pleistocene climate transition. *Science* **337**, 704–709 (2012).

[6] Menviel, L., Timmermann, A., Timm, O. E., and Mouchet, A. Deconstructing the Last Glacial termination: the role of millennial and orbital-scale forcings. *Quaternary Science Reviews* **30**, 1155–1172 (2011).

[7] Rignot, E., Mouginot, J., and Scheuchl, B. Ice Flow of the Antarctic Ice Sheet. *Science* **333**, 1427–1430 (2011).

[8] Fretwell, P., Pritchard, H. D., Vaughan, D. G., Bamber, J. L., Barrand, N. E., Bell, R., Bianchi, C., Bingham, R. G., Blankenship, D. D., Casassa, G., et al. Bedmap2: improved ice bed, surface and thickness datasets for Antarctica. *The Cryosphere* **7**(1), 375–393 (2013).

[9] Thomas, I. D., King, M. A., Bentley, M. J., Whitehouse, P. L., Penna, N. T., Williams, S. D. P., Riva, R. E. M., Lavallee, D. A., Clarke, P. J., King, E. C., Hindmarsh, R. C. A., and Koivula, H. Widespread low rates of Antarctic glacial isostatic adjustment revealed by GPS observations. *Geophysical Research Letters* **38**, L22302 (2011).

[10] EPICA Community Members. One-to-one coupling of glacial climate variability in Greenland and Antarctica. *Nature* **444**, 195–197 (2006).

[11] Sasgen, I., Mulvaney, R., Klemann, V., and Wolf, D. Glacial-isostatic adjustment and sea-level change near Berkner Island, Antarctica. Technical report, GeoForschungsZentrum Potsdam, Scientific Technical Report STR 07/05, (2005).

[12] Neumann, T. A., Conway, H., Price, S. F., Waddington, E. D., Catania, G. A., and Morse, D. L. Holocene accumulation and ice sheet dynamics in central West Antarctica. *Journal of Geophysical Research* **113**, F02018 (2008).

[13] Steig, E., Fastook, J., Zweck, C., Goodwin, I., Licht, K., White, J., and Ackert, R. J. West Antarctic Ice Sheet elevation changes. In The West Antarctic Ice Sheet: Behavior and environments, Alley, R. and Bindschadler, R., editors, volume 77, 75–90. American Geophysical Union Antarctic Research Series (2001).

[14] Waddington, E., Conway, H., Steig, E., Alley, R., Brook, E., Taylor, K., and White, J. Decoding the dipstick: Thickness of Siple Dome, West Antarctica, at the last glacial maximum. *Geology* **33**(4), 281 (2005).

[15] Steig, E. J., Morse, D. L., Waddington, E. D., Stuiver, M., Grootes, P. M., Mayewski, P. A., Twickler, M. S., and Whitlow, S. I. Wisconsinan and Holocene climate history from an ice core at Taylor Dome, western Ross Embayment, Antarctica. *Geografiska Annaler* **82**, 213–235 (2000).

[16] Parrenin, F., Barnola, J.-M., Beer, J., Blunier, T., Castellano, E., Chappellaz, J., Dreyfus, G., Fischer, H., Fujita, S., Jouzel, J., Kawamura, K., Lemieux-Dudon, B., Loulergue, L., Masson-Delmotte, V., Narcisi, B., Petit, J.-R., Raisbeck, G., Raynaud, D., Ruth, U., Schwander, J., Severi, M., Spahni, R., Steffensen, J. P., Svensson, A., Udisti, R., Waelbroeck, C., and Wolff, E. The EDC3 chronology for the EPICA Dome C ice core. *Climate of the Past* **3**, 485–497 (2007).

[17] Lorius, C., Raynaud, D., Petit, J., Jouzel, J., and Merlivat, L. Late Glacial Maximum-Holocene atmospheric and ice-thickness changes from Antarctic ice-core studies. *Annals of Glaciology* **5**, 88–94 (1984).

[18] Delmotte, M., Raynaud, D., Morgan, V., and Jouzel, J. Climatic and glaciological information inferred from air-content measurements of a Law Dome (East Antarctica) ice core. *Journal of Glaciology* **45**, 255–263 (1999).